

## Supporting Information

### **Single-Molecule Conformation Modulating Crystalline Polymorph of Physical $\pi$ - $\pi$ Pyrene Dimer: Blue and Green Emission of Pyrene Excimer**

*Wenzhe Jiang,<sup>a</sup> Yue Shen,<sup>a</sup> Yunpeng Ge,<sup>a</sup> Changjiang Zhou,<sup>a</sup> Yating Wen,<sup>a</sup> Haichao Liu,<sup>a,\*</sup> Hui Liu,<sup>a</sup> Shitong Zhang,<sup>a,b</sup> Ping Lu<sup>a</sup> and Bing Yang<sup>a,\*</sup>*

<sup>a</sup> State Key Laboratory of Supramolecular Structure and Materials, Jilin University, Changchun, 130012, P. R. China

<sup>b</sup> Institute of Theoretical Chemistry, Jilin University, Changchun 130012, P. R. China

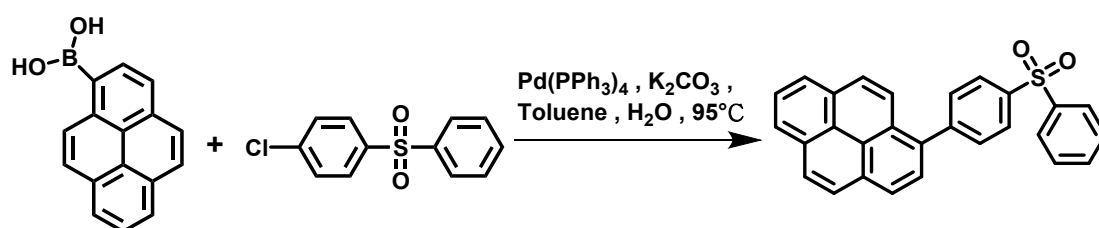
\*Corresponding Author. E-mail: hcliu@jlu.edu.cn, yangbing@jlu.edu.cn

<b>S-I Experimental Section</b> .....	S3
<i>Synthetic details of target molecule 1-DPS-PY</i> .....	S3
<i>General information</i> .....	S3
<i>Photophysical measurements</i> .....	S3
<i>Quantum chemical calculations</i> .....	S3
<i>Thermal stability measurements</i> .....	S3
<i>Electrochemical characterization</i> .....	S4
<i>Device fabrication and performances</i> .....	S4
<b>S-II Figures and Tables</b> .....	S5
<i>Fig. S1. PL spectra of powder and time-resolved fluorescence spectrum of powder</i> .....	S5
<i>Fig. S2. PL spectra and lifetime in various solution of 1-DPS-PY</i> .....	S5
<i>Fig. S3. PL spectra of 1-DPS-PY in THF/water mixtures with different water fractions</i> .....	S6
<i>Fig. S4. Time-resolved fluorescence spectra of crystals</i> .....	S6
<i>Table S1. Crystal data and refinement data of crystals</i> .....	S7
<i>Fig. S5. PL spectra and time-resolved fluorescence spectrum of 1-DPS-PY in doped PMMA film</i> .....	S8
<i>Fig. S6. Diagram of intermolecular interactions in crystals</i> .....	S8
<i>Fig. S7. Arrangement and interactions of crystals</i> .....	S8
<i>Fig. S8. Molecular ground-state geometry of 1-DPS-PY</i> .....	S9
<i>Fig. S9. Theoretical calculations of 1-DPS-PY</i> .....	S9
<i>Fig. S10. Theoretical calculations of dimers</i> .....	S9
<i>Fig. S11. The labels of atoms of dimers in crystals</i> .....	S10
<i>Fig. S12. PL spectra and time-resolved fluorescence spectrum of pure film and device E</i> .....	S10
<i>Fig. S13 Time-resolved spectra of purely evaporated film of 1-DPS-PY</i> .....	S10
<i>Fig. S14. Thermal properties of 1-DPS-PY</i> .....	S11
<i>Table S2. EL characteristics of devices in previous work</i> .....	S12
<b>S-III Reference</b> .....	S13

## S-I Experimental Section

### Materials

**Synthesis of 1-(*p*-Diphenylsulfone)Pyrene (1-DPS-PY).** A mixture of 1-pyrenylboronic acid (1.5 g, 6.10 mmol), 1-chloro-4-(phenylsulfonyl)benzene (1.0 g, 3.96 mmol), tetrakis(triphenylphosphine)palladium(0) ( $\text{Pd}(\text{PPh}_3)_4$ ) (200 mg, 0.173 mmol),  $\text{K}_2\text{CO}_3$  (5.0 g, 36.23 mmol), 18 ml  $\text{H}_2\text{O}$  and 27 ml toluene was degassed and recharged with nitrogen. After stirred and refluxed at  $95^\circ\text{C}$  for 48 h under nitrogen atmosphere, the mixture was washed with distilled water and then extracted with dichloromethane. The organic phase was dried with anhydrous sodium sulfate, filtered and concentrated in vacuum. It was purified via silica gel chromatography to afford the yellow solid (1.32 g, yield  $\sim 80\%$ ).  $^1\text{H}$  NMR (500 MHz,  $\text{DMSO-d}_6$ ,  $25^\circ\text{C}$ , TMS)  $\delta$  8.38 (dd,  $J = 14.4, 7.7$  Hz, 2H), 8.33 (d,  $J = 7.6$  Hz, 1H), 8.27 (d,  $J = 1.8$  Hz, 2H), 8.20 (dd,  $J = 8.8, 2.8$  Hz, 3H), 8.16 – 8.07 (m, 3H), 8.04 (t,  $J = 8.2$  Hz, 2H), 7.96 – 7.86 (m, 2H), 7.77 (t,  $J = 7.4$  Hz, 1H), 7.71 (t,  $J = 7.6$  Hz, 2H);  $^{13}\text{C}$  NMR (125 MHz,  $\text{CDCl}_3$ ,  $25^\circ\text{C}$ , TMS):  $\delta = 146.596$  (C), 141.743 (C), 140.391 (C), 135.327 (C), 133.301 (CH), 131.457 (CH), 131.290 (C), 130.828 (C), 129.409 (CH), 128.341 (C), 128.190 (CH), 128.054 (CH), 127.851 (CH), 127.777 (CH), 127.292 (CH), 127.280 (CH), 126.279 (CH), 125.598 (CH), 125.255 (CH), 124.293 (C), 124.711 (CH), 124.383 (CH); MALDI-TOF MS (mass  $m/z$ ): 418.46 [M $^+$ ]; Anal. calcd for  $\text{C}_{28}\text{H}_{18}\text{O}_2\text{S}$ : C 80.36, H 4.34, O 7.65, S 7.66; found: C 80.15, H 4.31, O 7.68, S 7.71



*Scheme S1. Synthetic details of target molecule 1-DPS-PY.*

### Measurements and Characterization

**General information.** The  $^1\text{H}$  and  $^{13}\text{C}$  NMR spectra were recorded on AVANCE 500 spectrometers at 298 K by utilizing deuterated dimethyl sulfoxide (DMSO) as solvents and tetramethylsilane (TMS) as a standard. The compounds were characterized by a Flash EA 1112, CHNS-O elemental analysis instrument. The MALDI-TOF-MS mass spectra were recorded using an AXIMA-CFR<sup>TM</sup> plus instrument.

**Photophysical measurements.** UV-vis absorption spectra were recorded on a UV-3100 spectrophotometer. Fluorescence measurements were carried out with a RF-5301PC. PL efficiency of solids and film was measured on the quartz plate using an integrating sphere apparatus with a FLS 920 spectrophotometer. PL efficiencies in solvents were measured using a UV-3100 and a RF-5301PC, with 0.1 mol  $\text{L}^{-1}$   $\text{H}_2\text{SO}_4$  solution of quinine sulfate as reference ( $\eta_{\text{PL}} = 54.6\%$ ). Time-resolved spectrum was measured and fitted with a FLS 980 spectrophotometer.

**Quantum chemical calculations.** All density functional theory (DFT) calculations were carried out using Gaussian 09 (version D.01) package on a PowerLeader cluster.<sup>1</sup> The ground-state geometry was fully optimized using B3LYP/6-31G(d, p). The excited-state geometries and emission properties were obtained using TD-M062X/6-31G(d, p) at the excited state geometry.

**Thermal stability measurements.** Thermal gravimetric analysis (TGA) was undertaken on a PerkinElmer thermal analysis system at a heating rate of 10 °C min<sup>-1</sup> and a nitrogen flow rate of 80 mL min<sup>-1</sup>. Differential scanning calorimetry (DSC) analysis was carried out using a NETZSCH (DSC-204) instrument at 10 °C min<sup>-1</sup> while flushing with nitrogen.

**Electrochemical characterization.** Cyclic voltammetry (CV) was performed with a BAS 100W Bioanalytical Systems, using a glass carbon disk ( $\Phi = 3$  mm) as the working electrode, a platinum wire as the auxiliary electrode with a porous ceramic wick, Ag/Ag<sup>+</sup> as the reference electrode, standardized for the redox couple ferricinium/ferrocene. All solutions were purged with a nitrogen stream for 10 min before measurement. The procedure was performed at room temperature and a nitrogen atmosphere was maintained over the solution during measurements.

**Device fabrication and performance.** The EL device was fabricated by vacuum deposition of the materials at indium tin oxide (ITO) glass. HATCN was deposited at a rate of 0.1 Å s<sup>-1</sup>. All of the organic layers were deposited at a rate of 0.3 ~ 0.5 Å s<sup>-1</sup>. The cathode was deposited with LiF (1 nm) at a deposition rate of 0.1 Å s<sup>-1</sup> and then capping with Al metal (120 nm) through thermal evaporation at a rate of 4.0 Å s<sup>-1</sup>. The EL spectra and Commission International de L'Eclairage chromaticity (CIE) coordination of 1-DPS-PY device were measured by a PR650 spectra scan spectrometer. The luminance-current density-voltage characteristics were recorded simultaneously with the measurement of the EL spectra by combining the spectrometer with a Keithley model 2400 programmable voltage-current source. All measurements were carried out at room temperature under ambient conditions.

EQE was calculated according to the formula below:

$$EQE = \frac{\pi \cdot L \cdot e}{683 \cdot I \cdot h \cdot c} \cdot \frac{\int_{380}^{780} I(\lambda) \cdot \lambda d\lambda}{\int_{380}^{780} I(\lambda) \cdot K(\lambda) d\lambda}$$

where L (cd m<sup>-2</sup>) is the total luminance of device, I (A) is the current flowing into the EL device,  $\lambda$  (nm) is EL wavelength,  $I(\lambda)$  is the relative EL intensity at each wavelength and obtained by measuring the EL spectrum,  $K(\lambda)$  is the CIE standard photopic efficiency function, e is the charge of an electron, h is the Planck's constant, c is the velocity of light.

## S-II Figures and Tables

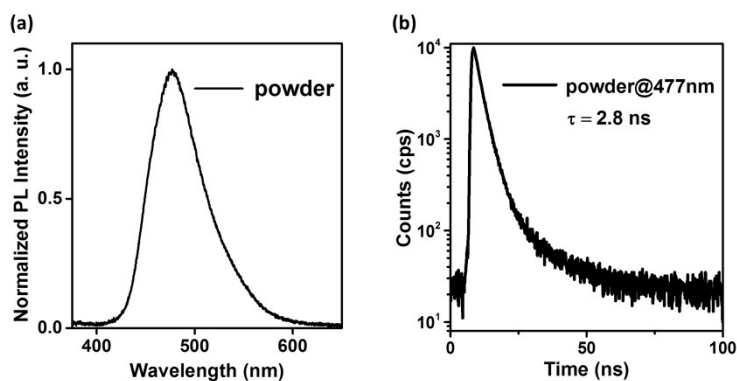


Fig. S1 (a) PL spectrum of 1-DPS-PY powder. (b) Time-resolved spectrum of 1-DPS-PY powder.

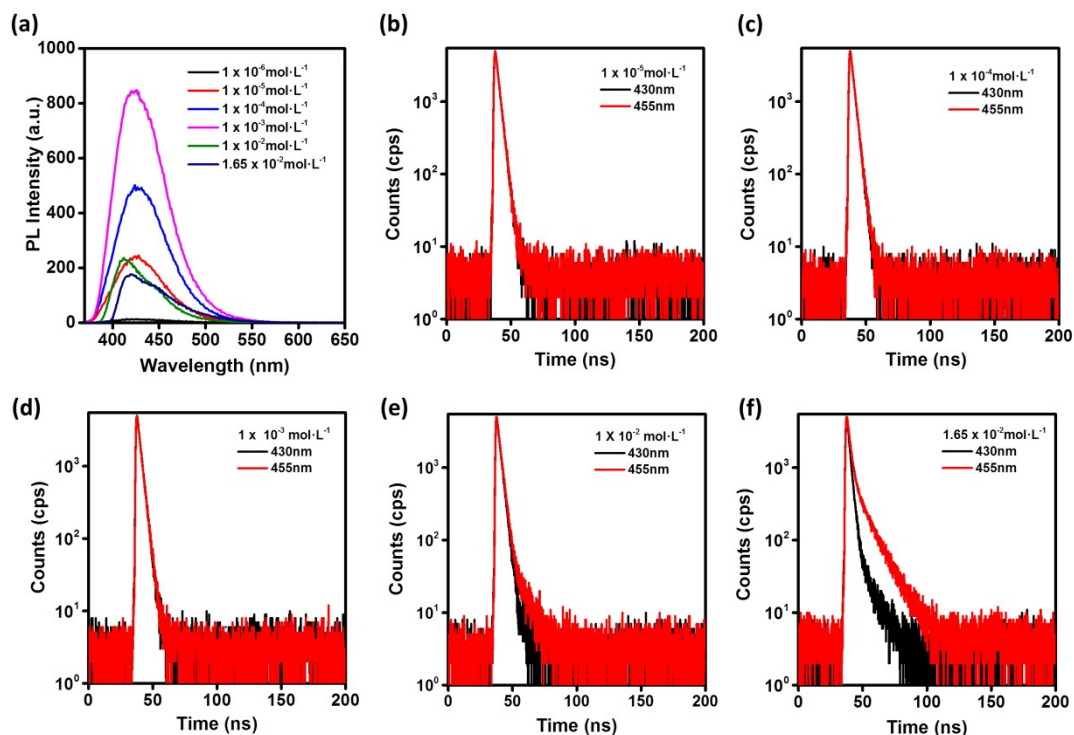
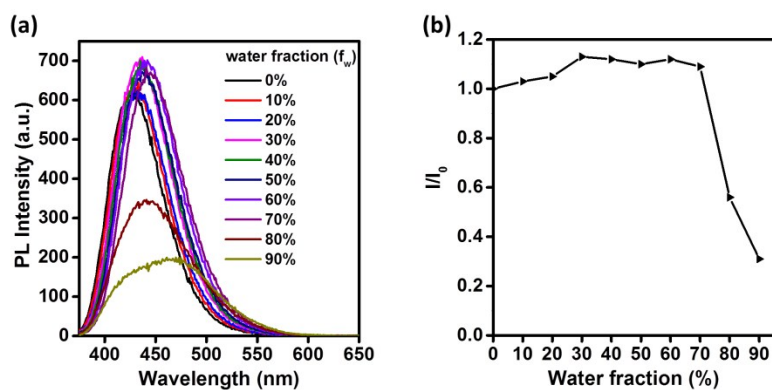


Fig. S2 (a) PL spectra of 1-DPS-PY in THF solutions. (b) ~ (e) Time-resolved spectra of 1-DPS-PY in THF solutions with various concentrations.

As concentration increases from  $1 \times 10^{-6}$  to  $1 \times 10^{-3}$  mol L<sup>-1</sup>, spectral intensity gradually increases because of the increasing molecular number; a further increasing concentration from  $1 \times 10^{-3}$  to  $1.65 \times 10^{-2}$  mol L<sup>-1</sup> results in a decreasing spectral intensity due to energy dissipation through the collision between molecules. High concentration of 1-DPS-PY in THF solution also induces the formation of pyrene excimer. In the high-concentration solution of  $1.65 \times 10^{-2}$  mol L<sup>-1</sup>, an obvious emission band around 455 nm was observed, probably originating from pyrene excimer. The lifetimes of excited state in various concentrations were further studied. From Fig. S2, in low-concentration solutions from  $1 \times 10^{-5}$  to  $1 \times 10^{-3}$  mol L<sup>-1</sup>, time-resolved spectra demonstrate a

single exponential decay at 430 and 455 nm in every solution. However, with the increase of concentration, time-resolved spectra exhibit a two-component lifetimes at 455 nm, which is longer compared to that at 430 nm. The appearance of two-component lifetimes at 455 nm indicates the excimer formation in the high-concentration solution.



**Fig. S3** (a) PL spectra of 1-DPS-PY in THF/water mixtures with different water fractions ( $f_w$ ). (b) Plot of relative PL intensity ( $I/I_0$ ) versus  $f_w$  of THF/water mixture of 1-DPS-PY, where  $I_0$  is the PL intensity in pure THF solution.

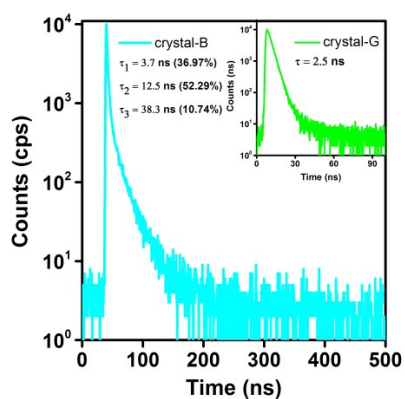
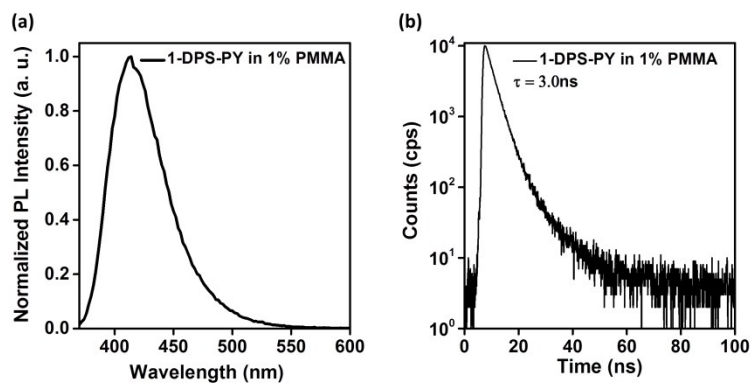


**Fig. S4** Time-resolved fluorescence spectra of crystal-G (2.5 ns) and crystal-B ( $\tau_1 = 3.7$  ns (36.97%),  $\tau_2 = 12.5$  ns (52.29%),  $\tau_3 = 38.3$  ns (10.74%)).

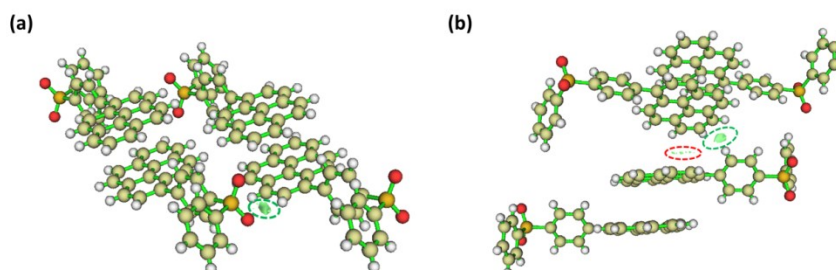
**Table S1.** Crystal data and refinement data of crystal-G and crystal-B.

	1-DPS-PY	
crystal color	yellow	colorless
empirical formula	C <sub>28</sub> H <sub>18</sub> O <sub>2</sub> S	C <sub>28</sub> H <sub>18</sub> O <sub>2</sub> S
formula weight	418.48	418.48
<i>T</i> [K]	293(2)	293(2)
crystal system	monoclinic	monoclinic
space group	P 21/n	P -1
<i>a</i> [Å]	14.6795(5)	8.8214(7)
<i>b</i> [Å]	9.4501(3)	9.7066(8)
<i>c</i> [Å]	15.2127(5)	13.2635(10)
$\alpha$ [°]	90.00	106.136(3)
$\beta$ [°]	103.0320(3)	98.153(3)
$\gamma$ [°]	90.00	106.332(3)
<i>V</i> [Å <sup>3</sup> ]	2055.99(12)	1016.69(14)
<i>Z</i>	4	2
F(000)	1054.0	436.0
density [g/cm <sup>3</sup> ]	1.352	1.367
$\mu$ [mm <sup>-1</sup> ]	0.181	0.183
reflections collected	23657	18050
unique reflections	4624	3585
<i>R</i> (int)	0.0510	0.0441
GOF	1.022	1.219
<i>R</i> <sub>1</sub> [ <i>I</i> > 2 $\sigma$ ( <i>I</i> )]	0.0511	0.0686
$\omega R$ <sub>2</sub> [ <i>I</i> > 2 $\sigma$ ( <i>I</i> )]	0.1099	0.2051
<i>R</i> <sub>1</sub> (all data)	0.0885	0.0888

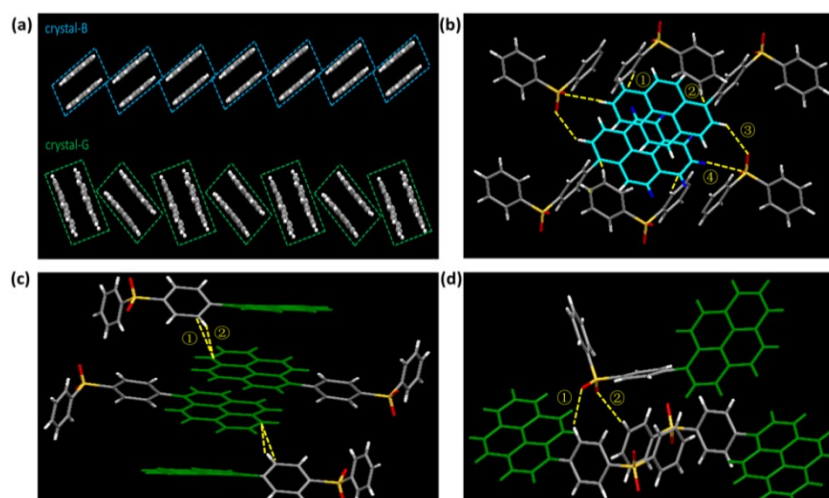
$\omega R_2$ (all data)	0.1301	0.2150
CCDC number	1969334	1969333



**Fig. S5** (a) PL spectrum of 1-DPS-PY in doped PMMA film. (b) Time-resolved spectrum of 1-DPS-PY in doped PMMA film.



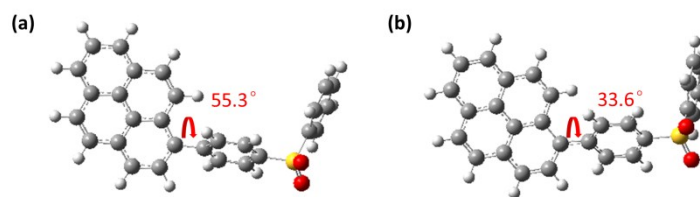
**Fig. S6** Diagram of intermolecular interactions in (a) crystal-B and (b) crystal-G by Multiwfn software.<sup>2</sup>



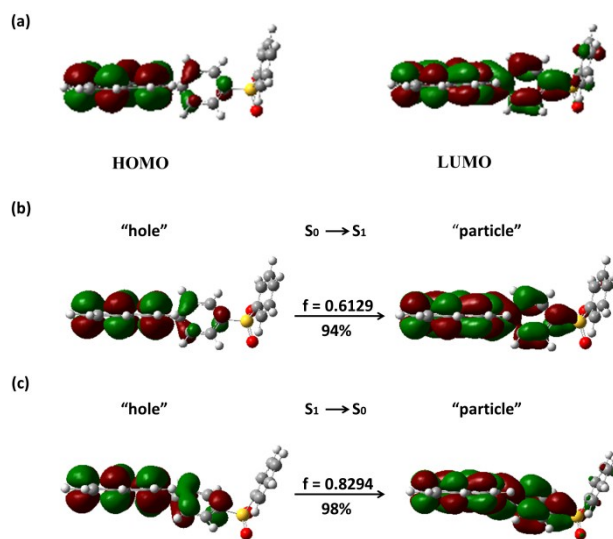
**Fig. S7** (a) Arrangement of crystal-B and crystal-G. (b) Interactions between pyrene moieties and diphenylsulfone in crystal-B (① : 2.284 Å, ② : 2.898 Å, ③ : 2.598 Å, ④ : 2.706 Å). (c) Interactions between pyrene moieties and diphenylsulfone in crystal-G.



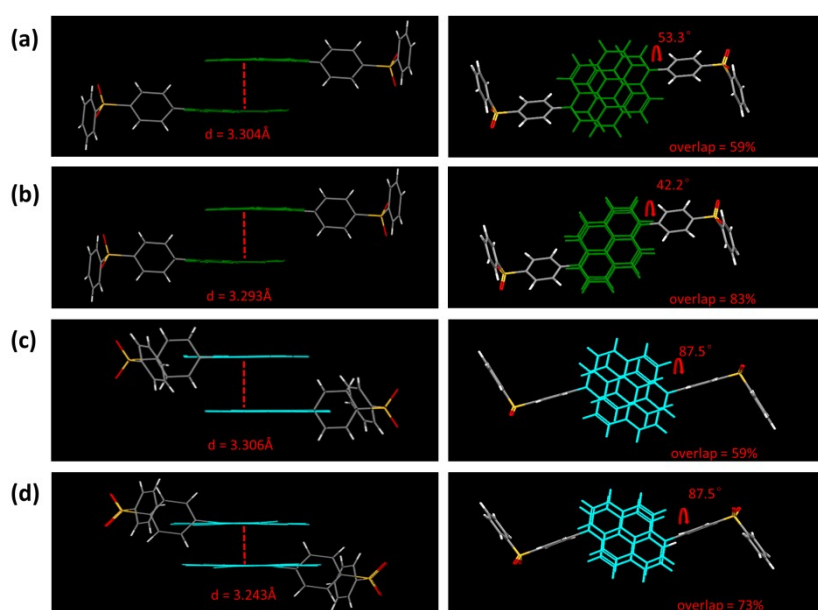
diphenylsulfone in crystal G (① : 3.386 Å, ② : 2.843 Å). (d) Interactions between diphenylsulfone in crystal G (① : 2.678 Å, ② : 2.565 Å).



**Fig. S8** (a) Molecular ground-state geometry of 1-DPS-PY. (b) Molecular excited-state geometry of 1-DPS-PY.

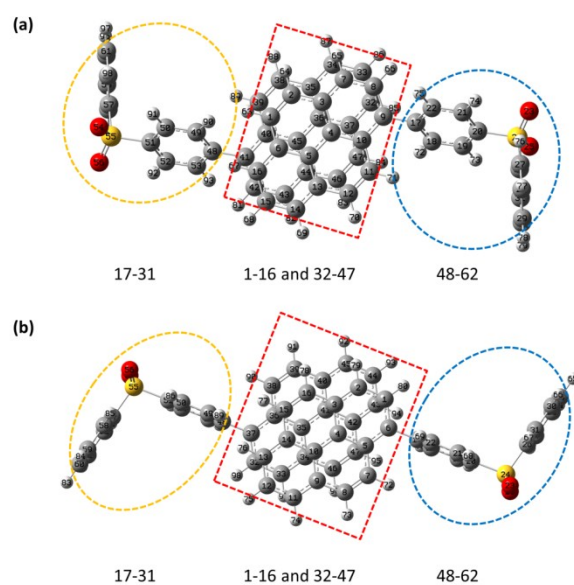


**Fig. S9** (a) HOMO and LUMO of 1-DPS-PY. (b) NTO for  $S_0 \rightarrow S_1$  transition in 1-DPS-PY. Herein,  $f$  represents for the oscillator strength, and the percentage weights of hole-particle are given for the  $S_0 \rightarrow S_1$  absorption. (c) NTO for  $S_1 \rightarrow S_0$  transition in 1-DPS-PY. Herein,  $f$  represents for the oscillator strength, and the percentage weights of hole-electron are given for the  $S_1 \rightarrow S_0$  emission.

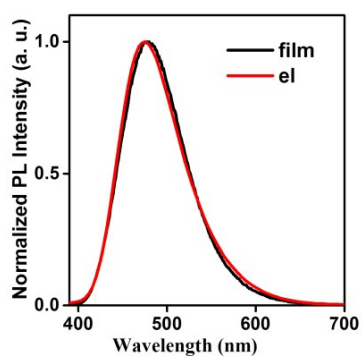


**Fig. S10** (a) Dimer geometry of crystal-G in the ground state. (b) Dimer geometry of crystal-G in the excited state.

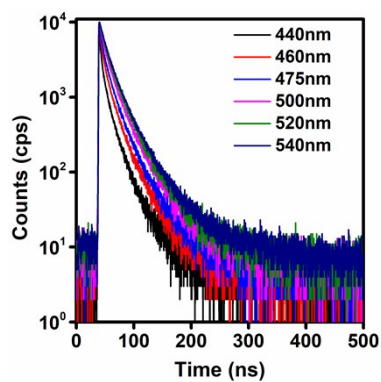
(c) Dimer geometry of crystal-B in the ground state. (d) Dimer geometry of crystal-B in the excited state.



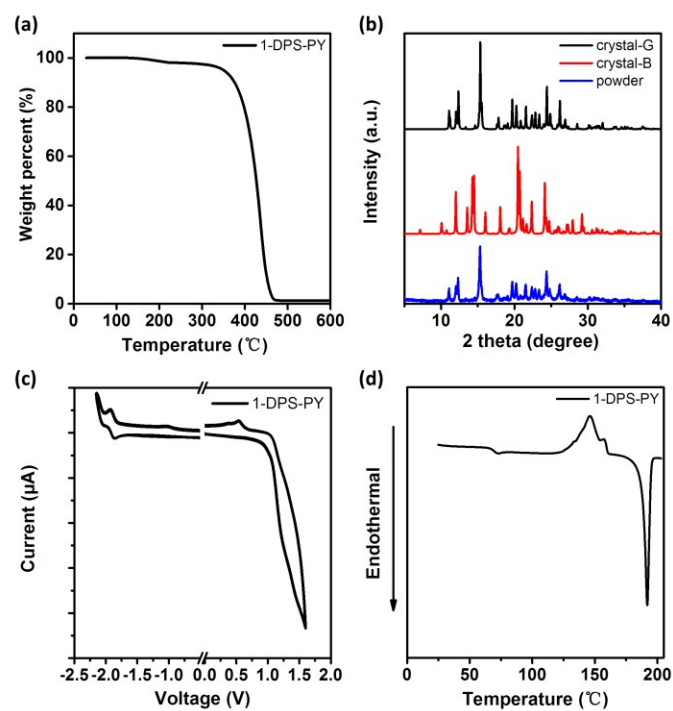
**Fig. S11** The labels of atoms of dimers in (a) crystal-G and (b) crystal-B.



**Fig. S12** PL spectrum of evaporated film and EL spectrum of device E.

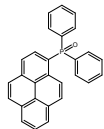
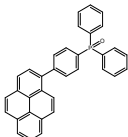
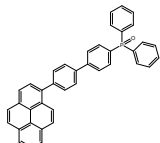
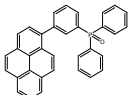
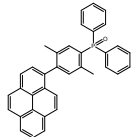
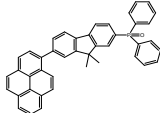
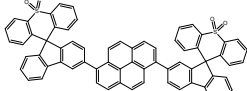
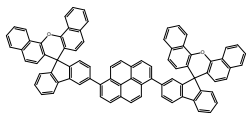
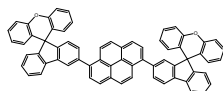
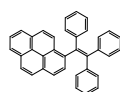
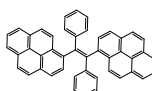


**Fig. S13** Time-resolved spectra of purely evaporated film of 1-DPS-PY.



**Fig. S14** (a) TGA curve of 1-DPS-PY. (b) XRD curves of 1-DPS-PY. (c) CV curves of 1-DPS-PY (HOMO = -5.68 eV; LUMO = -2.8 eV). (d) DSC curve of 1-DPS-PY.

**Table S2.** EL characteristics of devices in previous work.

device	compound	$\lambda_{el,max}$	CIE	CE	PE	EQE	$L_{max}$
		(nm)	(x,y)	(cd A <sup>-1</sup> )	(lm W <sup>-1</sup> )	(%)	(cd m <sup>-2</sup> )
Ref.62		491	(0.18,0.247)	14.6	7.65	3.3	23700
Ref.62		480	(0.15,0.385)	13.5	7.1	3.4	28440
Ref.62		476	(0.195,0.262)	15.75	8.24	3.8	33180
Ref.62		467	(0.168,0.227)	14.6	7.65	4.0	28440
Ref.62		465	(0.156,0.269)	8.86	4.46	3.0	15800
Ref.62		473	(0.185,0.237)	15.95	8.35	3.9	31200
Ref.60		466,519,560	(0.31,0.38)	4.52	3.10	1.68	10167
Ref.60		448,521,560	(0.34,0.43)	3.57	2.70	1.36	12162
Ref.60		468	(0.18,0.25)	5.94	3.8	3.16	21698
Ref.61		504	-	4.0	2.7	2.0	25470
Ref.61		516	-	10.2	9.2	3.3	49830

## S-III Reference

- [1] M. J. Frisch, G. W. Trucks, H. B. Schlegel, G. E. Scuseria, M. A. Robb, J. R. Cheeseman, G. Scalmani, V. Barone, B. Mennucci, G. A. Petersson, H. Nakatsuji, M. Caricato, X. Li, H. P. Hratchian, A. F. Izmaylov, J. Bloino, G. Zheng, J. L. Sonnenberg, M. Hada, M. Ehara, K. Toyota, R. Fukuda, J. Hasegawa, M. Ishida, T. Nakajima, Y. Honda, O. Kitao, H. Nakai, T. Vreven, J. A. Montgomery, Jr., J. E. Peralta, F. Ogliaro, M. Bearpark, J. J. Heyd, E. Brothers, K. N. Kudin, V. N. Staroverov, T. Keith, R. Kobayashi, J. Normand, K. Raghavachari, A. Rendell, J. C. Burant, S. S. Iyengar, J. Tomasi, M. Cossi, N. Rega, J. M. Millam, M. Klene, J. E. Knox, J. B. Cross, V. Bakken, C. Adamo, J. Jaramillo, R. Gomperts, R. E. Stratmann, O. Yazyev, A. J. Austin, R. Cammi, C. Pomelli, J. W. Ochterski, R. L. Martin, K. Morokuma, V. G. Zakrzewski, G. A. Voth, P. Salvador, J. J. Dannenberg, S. Dapprich, A. D. Daniels, O. Farkas, J. B. Foresman, J. V. Ortiz, J. Cioslowski, and D. J. Fox, *Gaussian 09, Revision D.01*, Gaussian, Inc., Wallingford CT, **2013**.
- [2] T. Lu and F. Chen, *J. Comput. Chem.*, 2012, **33**, 580-592.